

Rivelatori basati sulla ionizzazione

IONIZZAZIONE: indotta da particelle cariche: il passaggio delle particelle e' rivelato dalle ionizzazioni prodotte lungo il percorso della particella stessa.

Tecniche di visualizzazione di traccia

- Fondamentali nello sviluppo della fisica N. e SN. (inizialmente usando raggi cosmici poi presso acceleratori)
Ad es. nella scoperta di particelle con decadimento debole ($v.m. \tau \sim 10^{-10} s$) mediante osservazione decadimenti deboli con vertici di decadimento secondari a distanza misurabile ($c\tau \dots$)

Tecniche visualizzanti (traccia + ionizzazione/dE/dx) + campo magnetico (impulso)

Tecniche elettroniche

- Raccolta ionizzazione e trasformazione in impulso elettrico.
- Alla base di tutti i moderni rivelatori ed apparati

Rivelatori di Tracce

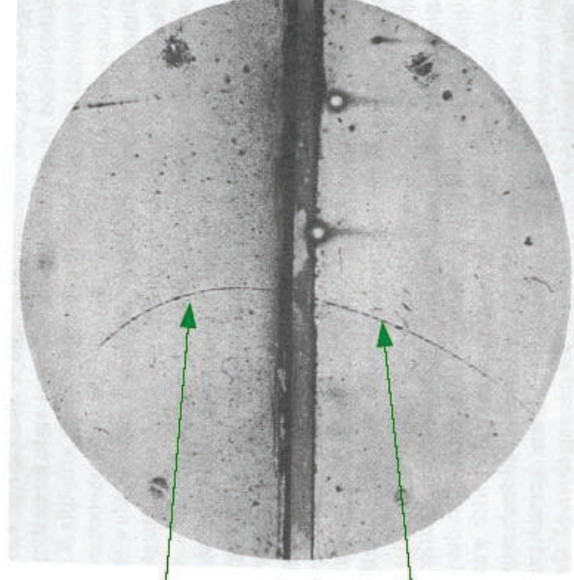
Tecniche di visualizzazione di traccia

1) **Camera a Nebbia (Wilson – 1912)** : un gas con **vapore sovrassaturo** produce goccioline dove sono presenti ioni a causa di una rapida espansione (asincrona nelle prime c.n., poi con trigger esterno). Si illumina e si fotografa la camera subito dopo l'espansione. Tipica risoluzione $\cong 0.5$ mm.

Molte informazioni da densita' ionizzazione (dE/dx) e curvatura (impulso) se campo magnetico presente

Camera a diffusione: camera a nebbia senza variazione di pressione

Anderson (1933)



23 MeV/c

6 mm Pb

63 MeV/c

- Intensita' traccia \rightarrow densita' ionizzazione (dE/dx)
- Curvatura \rightarrow impulso \rightarrow massa

Scoperta del Positrone



Evidenza particelle Lambda (Λ^0)

Misura traccia + ionizzazione (dE/dx)
+ campo magnetico (impulso)

Rochester et al Nature, 1947 Evidence for a new unstable particle

Proiettile: **Raggi cosmici** energetici (penetranti)
Rivelatore: camera a nebbia

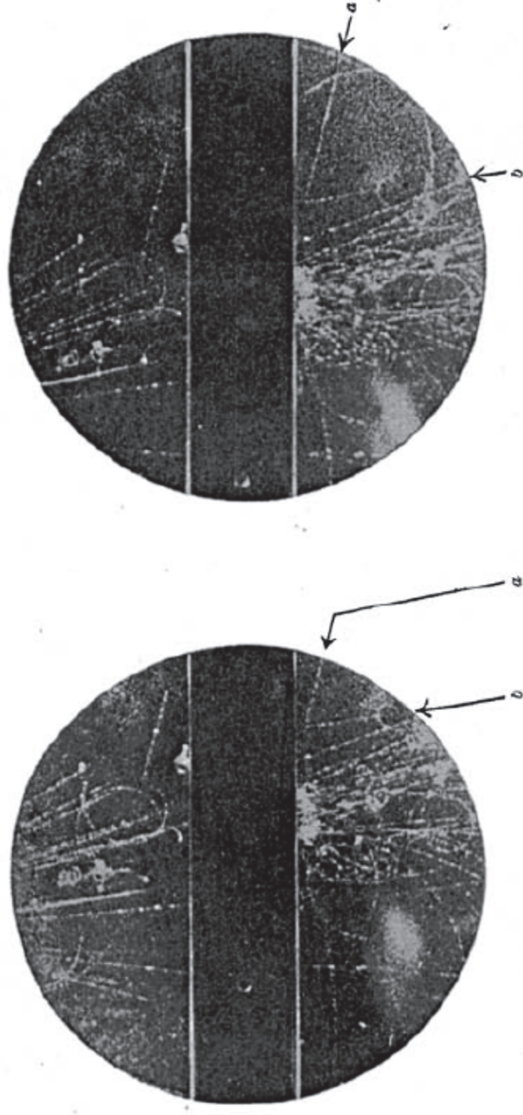


FIG. 1. STEREOGRAPHIC PHOTOGRAPHS SHOWING AN UNUSUAL FORK (a) IN THE GAS. THE DIRECTION OF THE MAGNETIC FIELD IS SUCH THAT A POSITIVE PARTICLE COMING FORWARDS IS DEVIATED IN AN ANTICLOCKWISE DIRECTION

Primi fasci ad acceleratori: BNL Cosmotron (π^-):
new Λ^0 evidence (Fowler et al)

Scoperta della stranezza

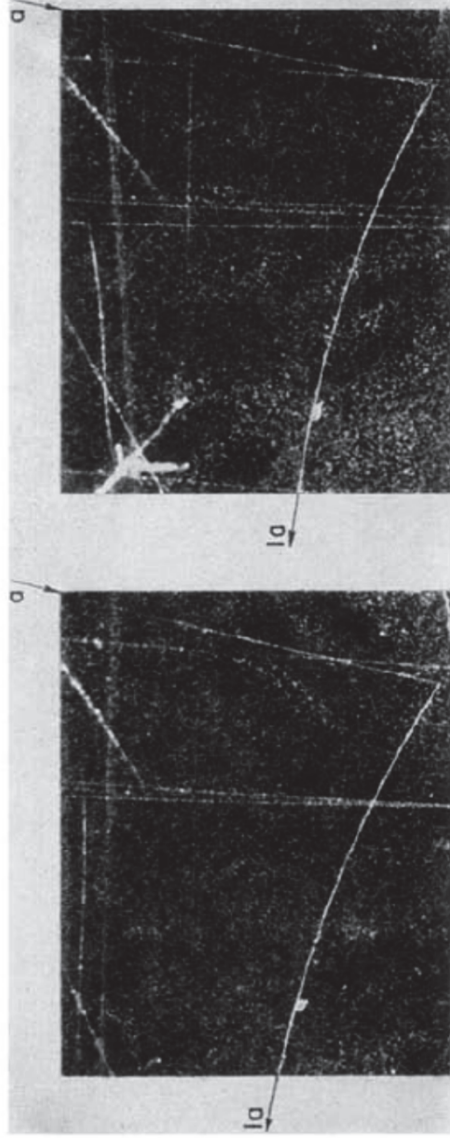


FIG. 4. Case F. Photograph of a negative unstable particle (a) best interpreted as a Λ^- . The decay product (1a) is identified as a π^- from momentum and ionization density.

These unstable particles were clearly produced with a large cross section, some percent of the cross section for producing ordinary particles, pions and nucleons. The puzzle was this: The new particles were produced in strong interactions and decayed into strongly interacting particles, but if the decays involved strong interactions, the particle lifetimes should have been ten orders of magnitude less than those observed...

Camera a nebbia: la nascita dell' antineutrino

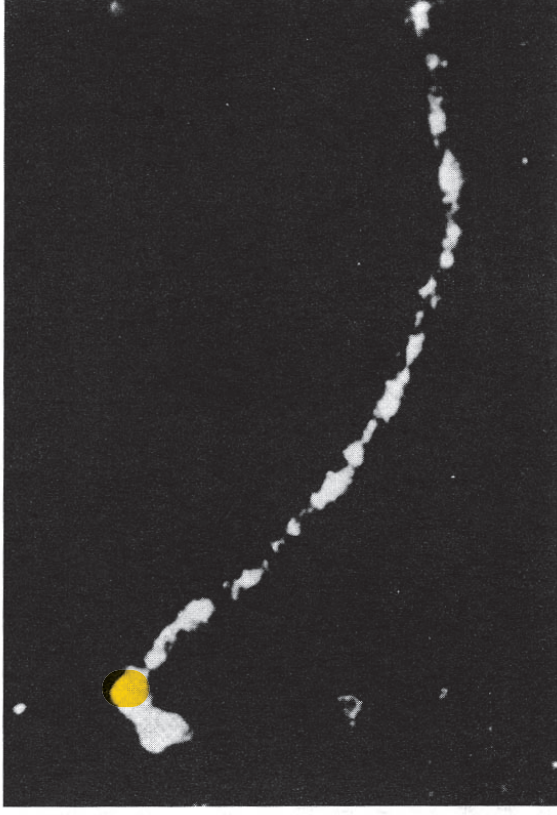


Fig. 1.1. Cloud chamber photograph of the birth of an antineutrino. It depicts the β -decay of the radioactive nucleus ${}^6\text{He} \rightarrow {}^6\text{Li} + e^- + \bar{\nu}_e + 3.5 \text{ MeV}$. The long track is that of the electron, the short thick track that of the recoiling ${}^6\text{Li}$ nucleus. Some momentum is missing, and has to be ascribed to an uncharged particle (an antineutrino) travelling upwards in the picture (after Csikay and Szalay 1957). The cloud chamber consists essentially of a glass-fronted cylindrical tank of gas saturated with water vapour. Upon applying a sudden expansion by means of a piston at the rear of the chamber, the gas cools adiabatically and becomes supersaturated. Water vapour therefore condenses as droplets, preferentially upon charged ions created, for example, by the passage of a charged particle through the gas. The cloud chamber was invented by C.T.R. Wilson for a quite different purpose: to try to reproduce, in the laboratory, the 'glory' phenomenon he had observed on a Scottish mountain top. Wilson failed in this endeavour but by 1912 had given the world a valuable new technique for nuclear research.

Rivelatori di Tracce

Tecniche di visualizzazione di traccia

2) Camera a Bolle (Glaser– 1952):
un liquido (idrogeno, deuterio, elio....)
in cui la **pressione idrostatica è**
mantenuta per qualche millisecondo **più**
bassa della sua tensione di vapore. Si
formano delle **bollicine** lungo la
traiettoria delle particelle a causa della
presenza delle coppie e-ione che
producono un aumento locale della
temperatura.

Risoluzione spaziale da 300 a 20 μm .

SCOPERTA ANTI- NEUTRONE:

$\text{anti-p} + \text{p} \rightarrow \text{anti-n} + \text{n}$

Annichilazione anti-n (stella con
energia maggiore di 1.5 GeV)

4. Antibaryons

83

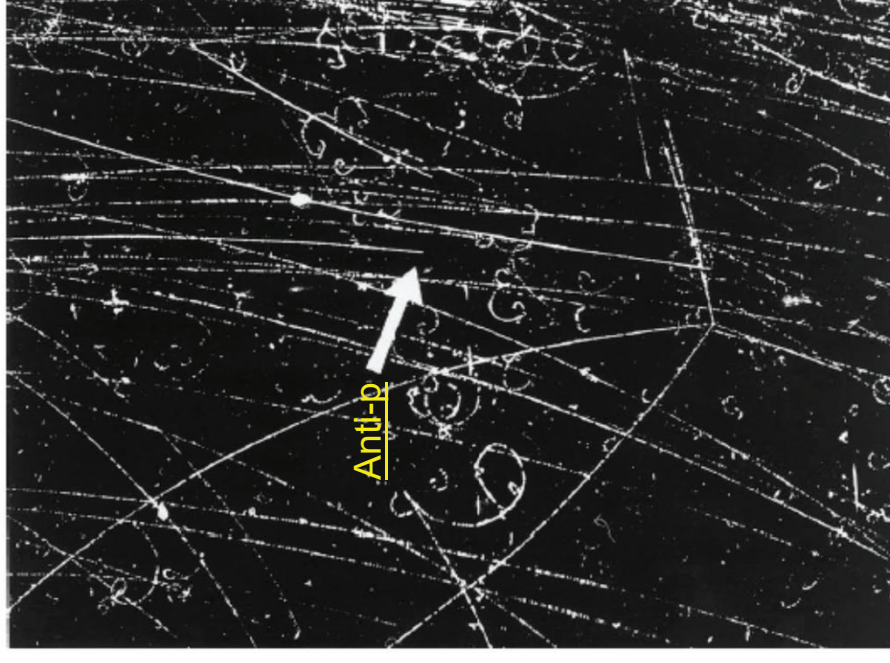


Figure 4.2. An antiproton enters the bubble chamber from the top. Its track disappears at the arrow as it charge exchanges, $p\bar{p} \rightarrow n\bar{n}$. The antineutron produces the star seen in the lower portion of the picture. The energy released in the star was greater than 1500 MeV. (Ref. 4.7)

Produzione di coppie in camera a bolle

$$\gamma (e) \rightarrow e^+ e^- (e)$$

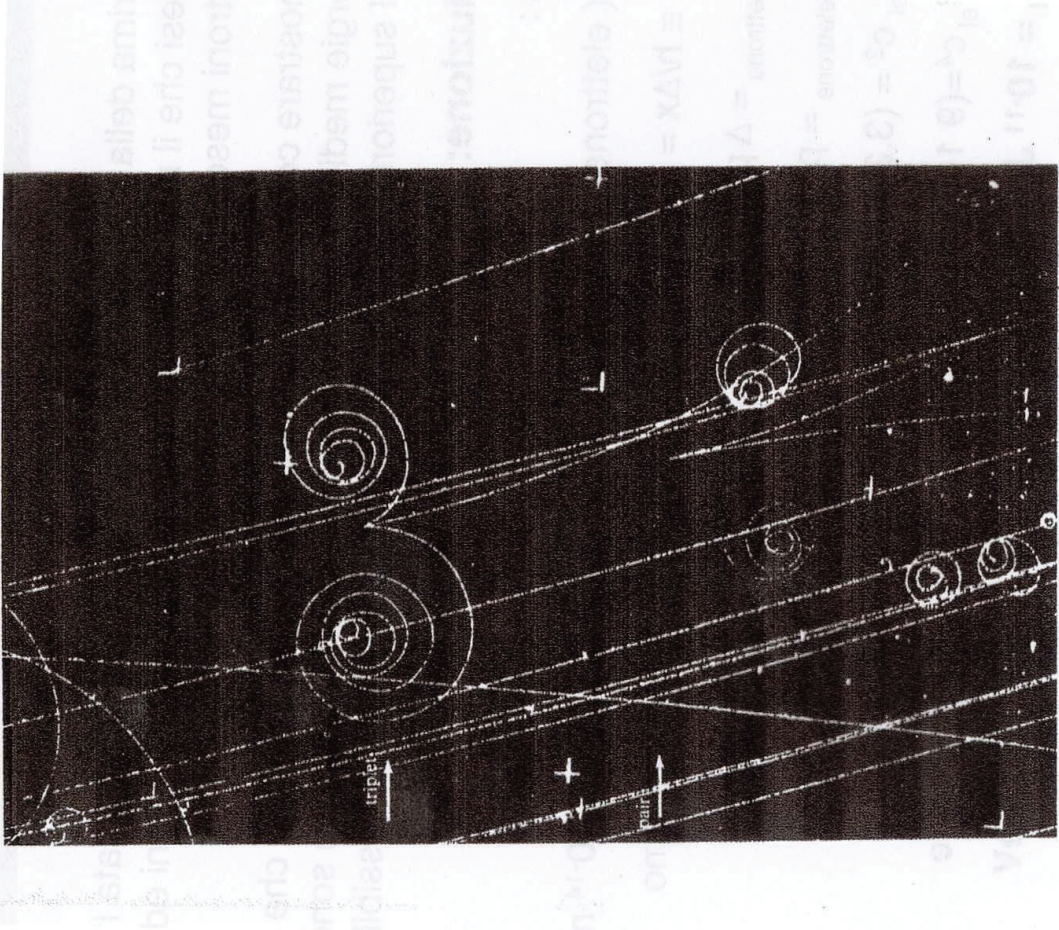


Figura 2.28. Formazione di una coppia elettrone-positrone nel campo di un elettrone (tripletto).
Formazione di una coppia nel campo di un protone (coppia). (Camera a bolle a idrogeno). [Fotografia gentilmente concessa dal Lawrence Radiation Laboratory].

The bubble chamber was invented by Donald Glaser in 1953. The first chambers used propane and other liquid hydrocarbons. The idea was rapidly adapted by Luis Alvarez and his group who used liquid hydrogen (and later also deuterium) as the working liquid. They also developed methods for building increasingly large chambers. The bubble chamber works by producing a superheated liquid by rapid expansion just before (about 10 ms) the arrival of the particles to be studied. Bubbles are formed when boiling starts around the ions produced by the passage of the charge particles through the liquid. These bubbles are allowed to grow for about 2 ms at which time lights are flashed and the bubbles are photographed. The properties of bubble chambers are ideally suited for use with accelerators. At an accelerator, the arrival time of a particle beam is known. This allows one to expand the chamber before the arrival of the charged particles, which is not possible in cosmic-ray experiments.

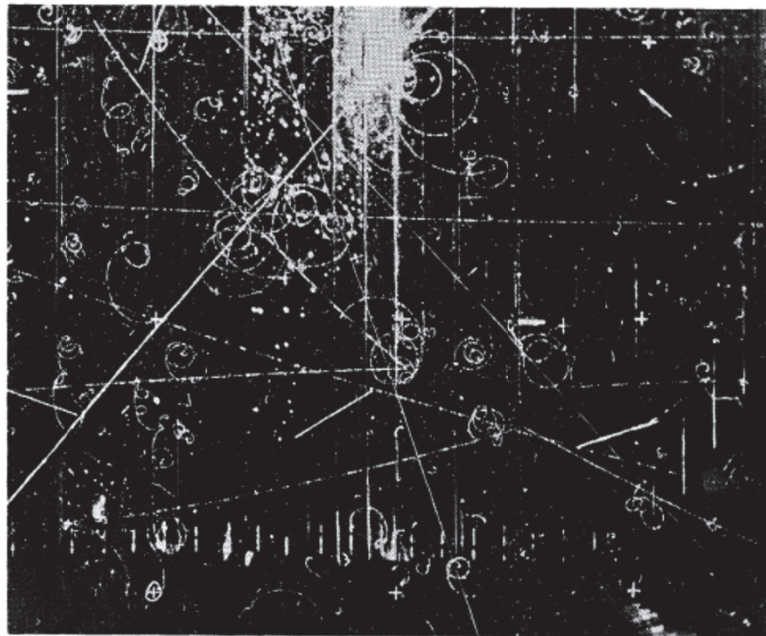
The discovery of the Ξ^0 did not take place until 1959. Since the Ξ has strangeness -2 , its production by pions is quite infrequent: the minimal process would be $\pi^- p \rightarrow K^0 K^0 \Xi^0$. A more effective means is to start with a particle with strangeness -1 . This was accomplished by L. Alvarez and co-workers using a hydrogen bubble chamber and a mass-separated beam of K^- mesons of momentum about 1 GeV/c produced by the Bevatron. Using the great analytical power of the bubble chamber technique, they were able to identify an event $K^- p \rightarrow K^0 \Xi^0$ (Ref. 3.20). The K^0 decayed into $\pi^+ \pi^-$. The Ξ^0 decayed into $\Lambda^0 \pi^0$. Both the decay of the K^0 and the decay of the Ξ^0 gave noticeable gaps in the bubble chamber pictures. The Λ^0 was identified by its charged decay mode, $\Lambda \rightarrow p \pi^-$. The last hyperon, Ω^- , was not discovered until 1964, as discussed in Chapter 5.

resonant frequency of the μ meson to that of the proton in water in the same magnetic field. The results for copper and aluminum are corrected by a rough calculation of the Knight shift⁶ and then agree with that for CHBr_3 in which there should be no diamagnetic shift to the accuracy quoted. It should be noted that our result for aluminum disagrees with that of the Chicago group^{4,7} to about twice their stated error.

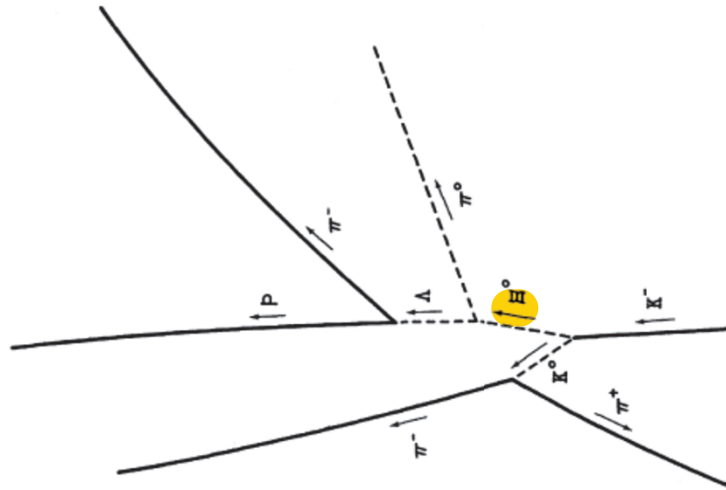
NEUTRAL CASCADE HYPERON EVENT*

Luis W. Alvarez, Philippe Eberhard,†
 Myron L. Good, William Graziano,
 Harold K. Ticho,‡ and Stanley G. Wojcicki
 Lawrence Radiation Laboratory
 and Department of Physics,
 University of California,
 Berkeley, California

(Received February 9, 1959)



(a)



(b)

FIG. 1. Photograph and sketch of Ξ^0 event.

cs10=uss

Camera a Bolle: scoperta anti- Λ

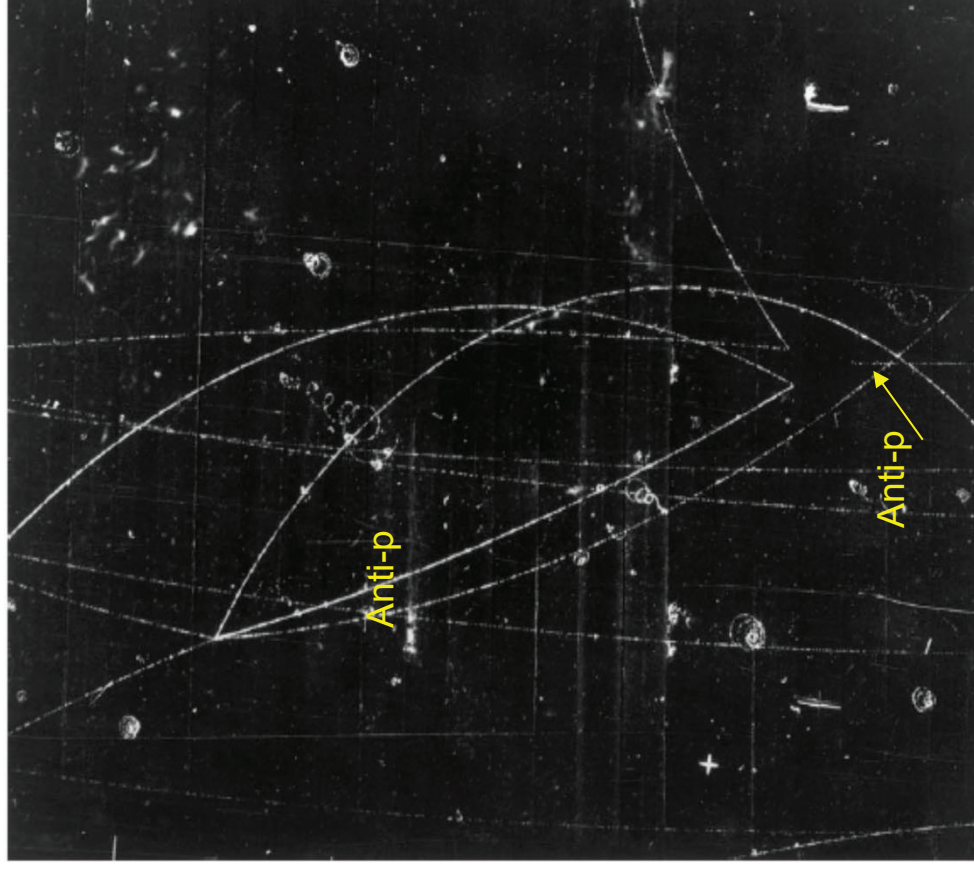


Figure 4.3. Production of a $\Lambda\bar{\Lambda}$ pair by an incident antiproton. The antiproton enters the chamber at the bottom and annihilates with a proton. The Λ and $\bar{\Lambda}$ decay nearby. The antiproton from the antilambda annihilates on the left-hand side of the picture and gives rise to a 4 prong star. The picture is from the 72-inch bubble chamber at the Bevatron. (Ref. 4.9)

Anti-p + p \rightarrow anti- Λ + Λ
(e successiva
annichilazione anti-p)
 $\Lambda \rightarrow \pi^- p$
Anti- $\Lambda \rightarrow \pi^+ \text{ anti-p}$

Scoperta di risonanze: Sigma(1385)

The full importance and wide-spread nature of resonances became clear only in 1960 when Luis Alvarez and a team that was to include A. Rosenfeld, F. Solmitz, and L. Stevenson began their work with separated K^- beams in hydrogen bubble chambers exposed at the Bevatron. The first resonance observed (Ref. 5.5) was the $I = 1$ $\Lambda\pi$ resonance originally called the Y_1^+ , but now known as the $\Sigma(1385)$. The reaction studied in the Lawrence Radiation Laboratory's 15-inch hydrogen bubble chamber was $K^-p \rightarrow \Lambda\pi^+\pi^-$ at 1.15 GeV/c. The tracks in the bubble chamber pictures were measured on semi-automatic measuring machines and the momenta were determined from the curvature and the known magnetic field. The measurements were refined by requiring that the fitted values conserve momentum and energy. The invariant masses of the pairs of particles,

$$M_{12}^2 = (p_1 + p_2)^2 = (E_1 + E_2)^2 - (\mathbf{p}_1 + \mathbf{p}_2)^2 \quad (5.8)$$

were calculated. For three-particle final states a Dalitz plot was used, with either the center-of-mass frame kinetic energies, or equivalently, two invariant masses squared, as variables. As for the τ -meson decay originally studied by Dalitz, in the absence of dynamical correlations, purely s-wave decays would lead to a uniform distribution over the Dalitz plot. The most surprising result found by the Alvarez group was a band of high event density at fixed invariant mass, indicating the presence of a resonance.

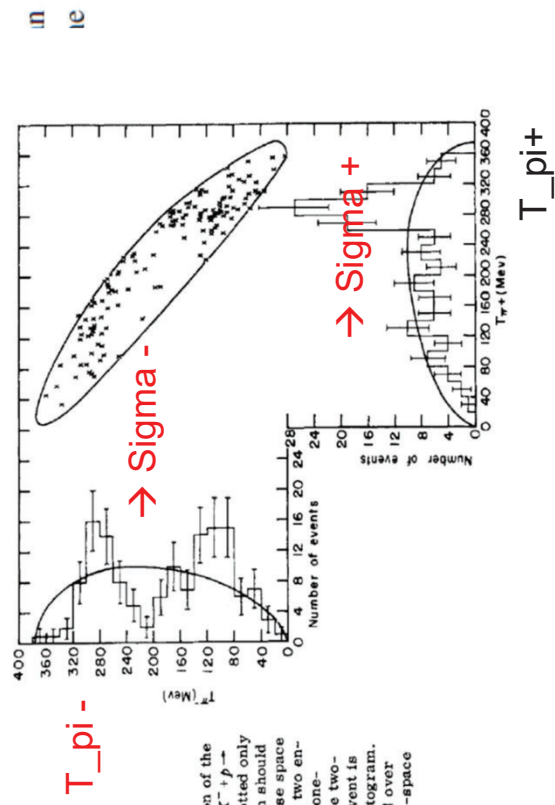


FIG. 1. Energy distribution of the two pions from the reaction $K^+ + p \rightarrow \Lambda + \pi^+ + \pi^-$. Each event is plotted only once on the Dalitz plot, which should be uniformly populated if phase space dominated the reaction. The two energy histograms are merely one-dimensional projections of the two-dimensional plot, and each event is represented once on each histogram. The solid lines superimposed over the histograms are the phase-space curves.

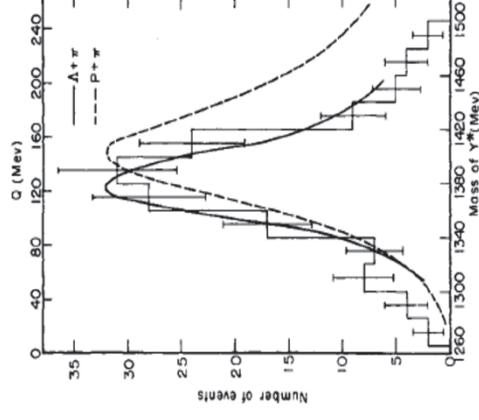


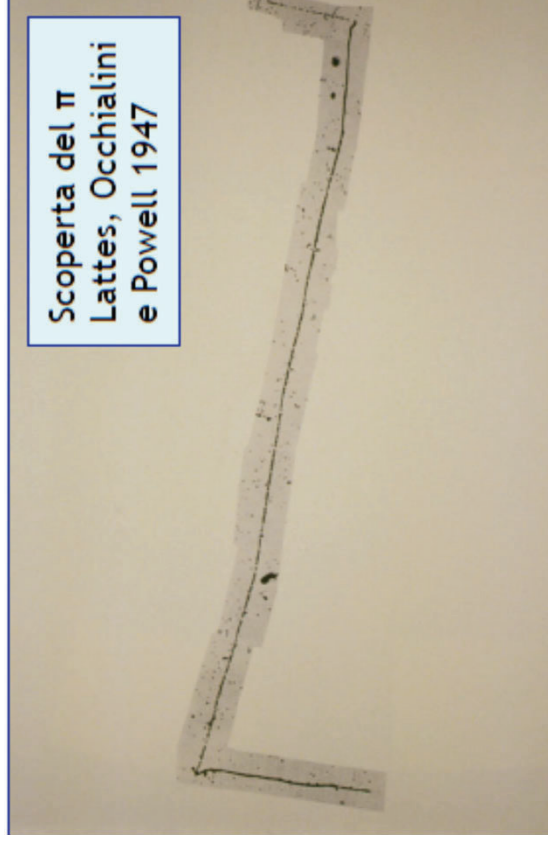
FIG. 2. Mass distribution for Y^* and fitted curves for $\pi\Lambda$ and $\pi\pi$ resonances. The lower scale refers only to the $\pi\Lambda$ resonance. Q is the kinetic energy released when either isobar dissociates. The curve for the $\pi\Lambda$ resonances is fitted to the center eight histogram intervals of our data. The $\pi\pi$ curve is the fit obtained by Gell-Mann and Watson⁷ to $\pi\pi$ scattering data. Both fits are to the formula $\sigma \propto k^2 \Gamma^2 / [(E - E_0)^2 + \Gamma^2]$, where $\Gamma = 2b(a/\lambda)^2 / [1 + (a/\lambda)^2]$.

Rivelatori di Tracce

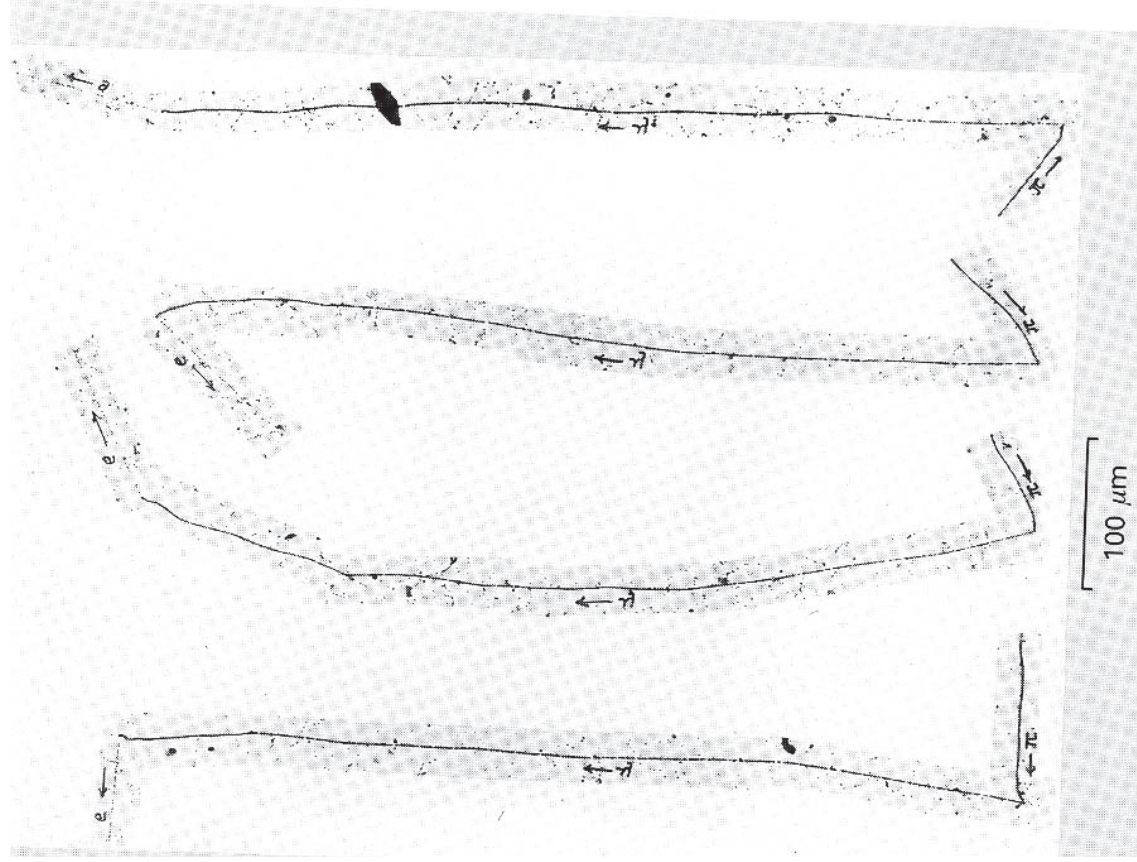
A) Tecniche Visualizzanti

3) **Emulsioni Nucleari (Powell– 1939):** costituite da grani di AgBr (bromuro di argento) immersi in gelatine con densità di alcuni grani / μm . La particella produce elettroni che trasformano i grani in Argento metallico.

Risoluzione spaziale $\cong 1 \mu\text{m}$.



Emulsioni: scoperta del pione carico



Anti-proton star

antiproton

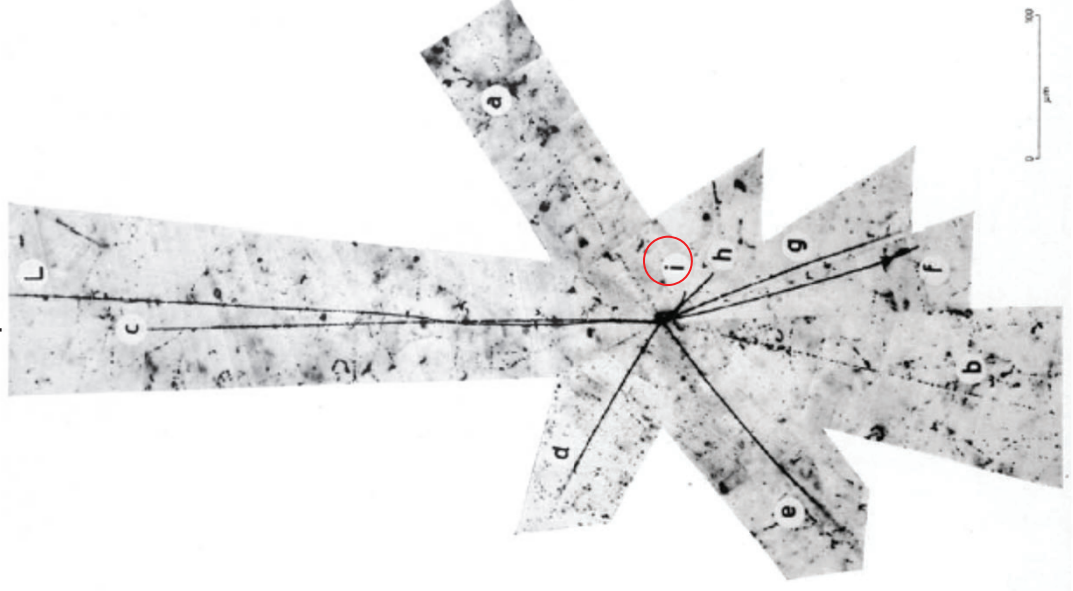


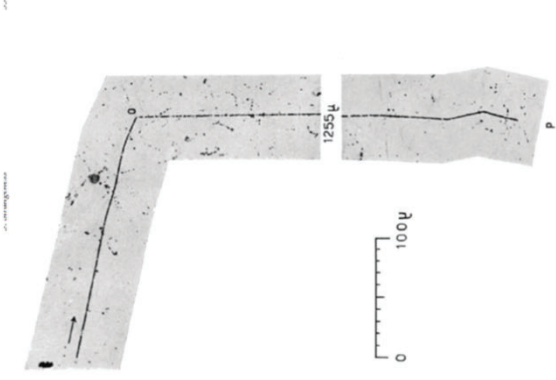
Figure 4.1. The first antiproton star observed in an emulsion. The incident antiproton is track *i*. The light tracks *a* and *b* are pions. Track *c* is a proton. The remaining tracks are protons or alpha particles. The exposure was made at the Bevatron. (Ref. 4.2)

Chamberlain et al, Phys. Rev 101 (1956)

Scoperta della stranezza:

Iperone $\Sigma^+ \rightarrow p \pi^0 \Rightarrow$

Scoperta ipernuclei



Observed by R. Levi-Strauss
Figure 3.4. An emission event with a Σ^+ entering from the left. The decay is $\Sigma^+ \rightarrow p \pi^0$. The f is observed to stop after 1255 μm. (Ref. 3.8)

(traccia f, creata dall'arrivo di un raggio cosmico su di un nucleo)

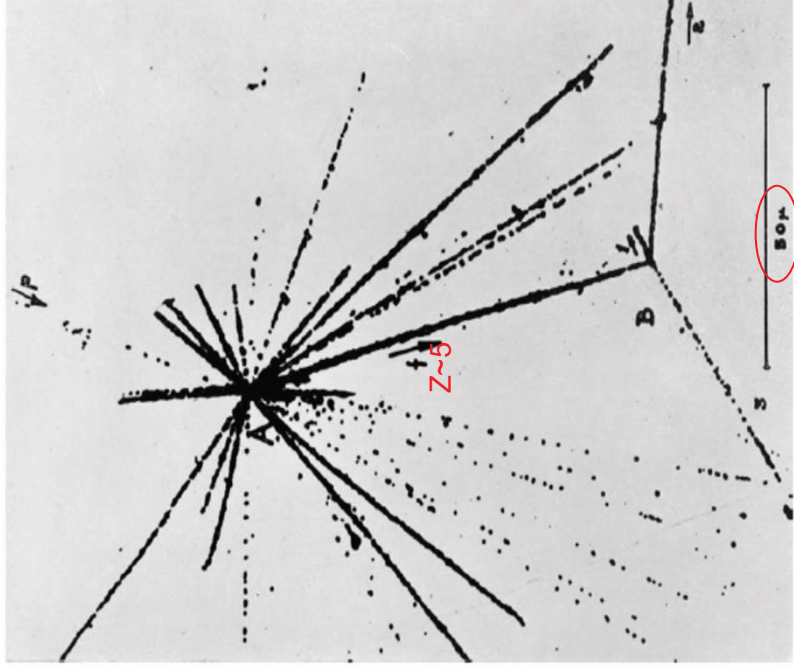


Figure 3.5. The star at A is caused by a cosmic-ray (marked p) incident from above colliding with a silver or bromine atom in the emulsion. The track f is due to a nuclear fragment with charge about 5. Its decay at point B shows that it contained a hyperon. The scale at the bottom indicates 50 μm. (Ref. 3.10)

Rivelatori di Tracce

4) **Camera a Scintille (1950)** [...primi passi verso rivelatori elettronici] lastre conduttrici separate di 1 cm connesse a tensione ed a massa in modo alternato ad un generatore IMPULSIVO di tensione. Tra le lastre vi è un gas NOBILE (He, Ne) che viene ionizzato dal passaggio della particella carica. Dopo il passaggio viene impulsato un campo elettrico di $\sim 10\text{KV/cm}$ che accelerando gli elettroni innesca una scarica lungo tutta la traccia di ionizzazione lasciata dalla particella. **Le scintille sono nel visibile e vengono fotografate.**

Risoluzione spaziale ≤ 1 mm.

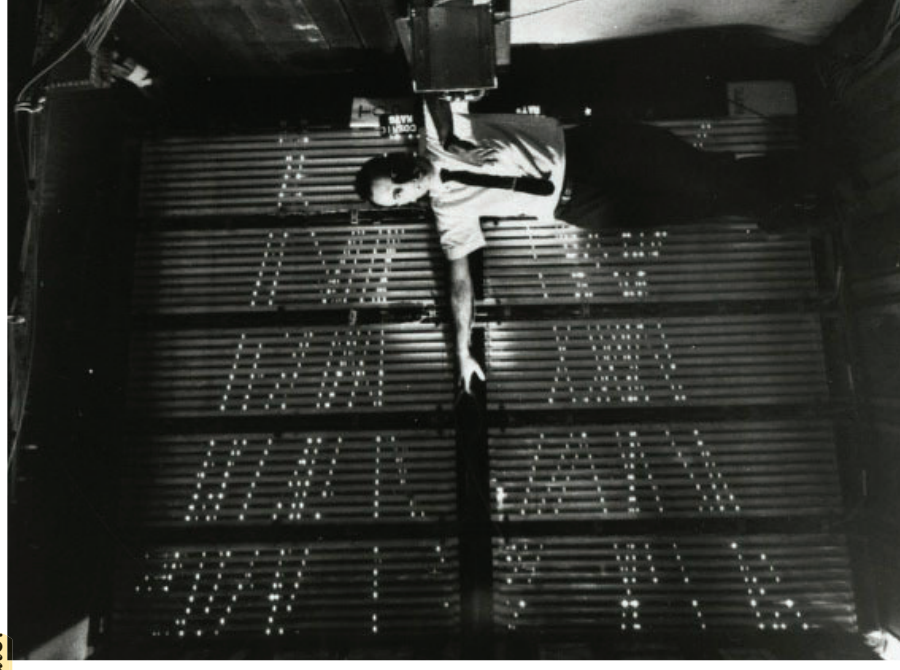
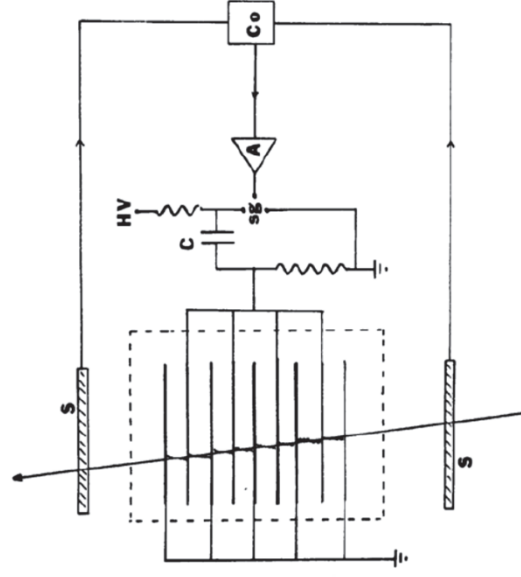


Figure 12.2 Principles of spark chamber operation. (S) Scintillation counter, (Co) coincidence circuit, (A) amplifier, and (sg) spark gap.



Melvin Schwartz one of the co-discoverers of the muon neutrino with a spark chamber used in its discovery.

Rivelatori di Tracce

4) **Camera a Scintille (1950)** [...primi passi verso rivelatori elettronici] lastre conduttrici separate di 1 cm connesse a tensione ed a massa in modo alternato ad un generatore IMPULSIVO di tensione. Tra le lastre vi è un gas NOBILE (He, Ne) che viene ionizzato dal passaggio della particella carica. Dopo il passaggio viene impulsato un campo elettrico di $\sim 10\text{KV/cm}$ che accelerando gli elettroni innesca una scarica lungo tutta la traccia di ionizzazione lasciata dalla particella. Le scintille sono nel visibile e vengono fotografate.

Risoluzione spaziale ≤ 1 mm.

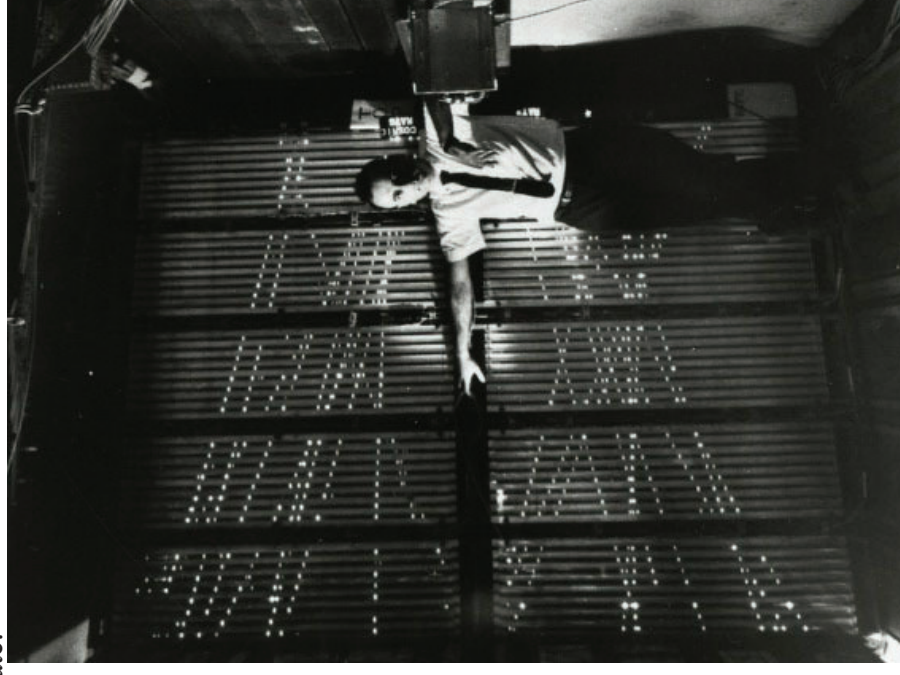
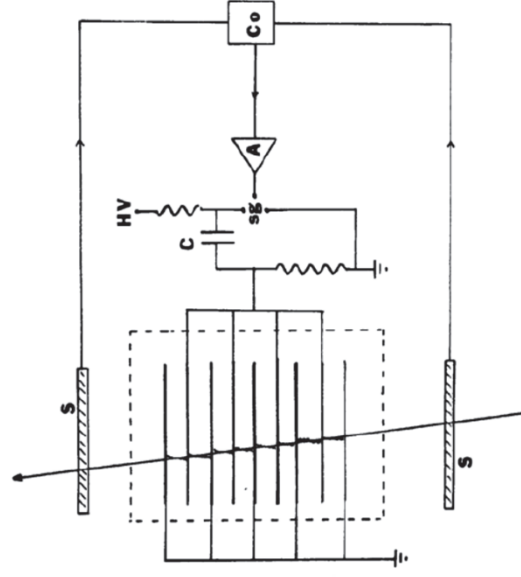


Figure 12.2 Principles of spark chamber operation. (S) Scintillation counter, (Co) coincidence circuit, (A) amplifier, and (sg) spark gap.



Melvin Schwartz one of the co-discoverers of the muon neutrino with a spark chamber used in its discovery.

Rivelatori di Tracce tramite ionizzazione

B) Tecniche Elettroniche

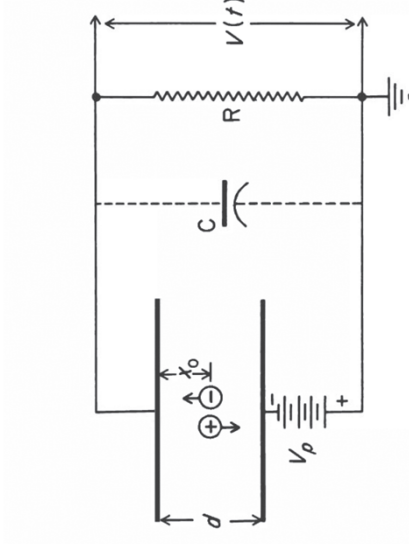
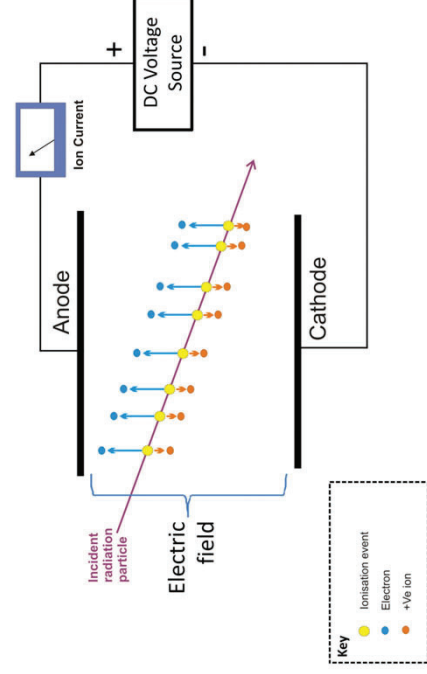
I rivelatori visualizzanti (c. nebbia, c.bolle,...) richiedono di **fotografare tutti gli eventi** e analizzarli in seguito. Sono pertanto sistemi **inefficienti e lenti**.

Nei rivelatori che utilizzano invece tecniche elettroniche, la carica elettrica, prodotto della ionizzazione dovuta al passaggio della particella, viene **raccolta con opportuni campi elettrici e trasformata in un segnale elettrico** che viene poi elaborato e salvato.

La modalita' di raccolta puo' essere **diretta** (camera a ionizzazione), **amplificata** mediante moltiplicazione della carica (camera proporzionale) o **saturata** (contatore Geiger)

Il materiale puo' essere **GAS, LIQUIDO o SOLIDO**.

Visualisation of ion chamber operation



Rivelatori di Tracce tramite ionizzazione

Varie tipologie (metodi, tecniche, geometrie,...):

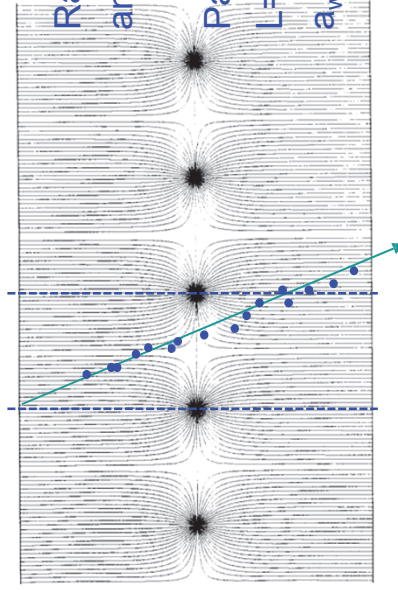
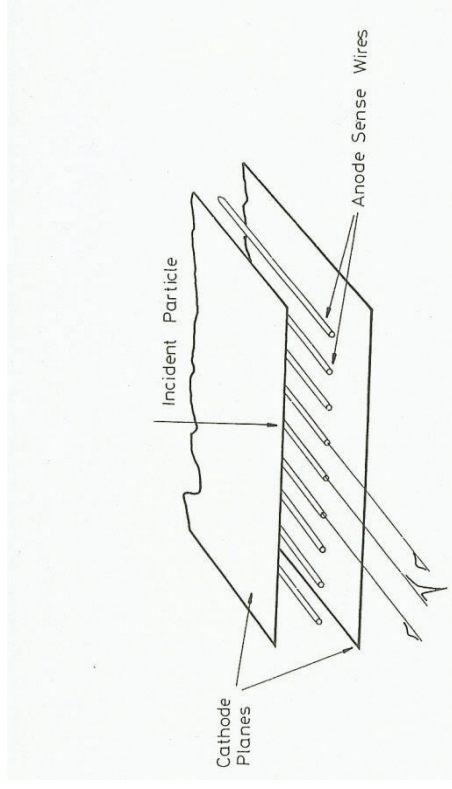
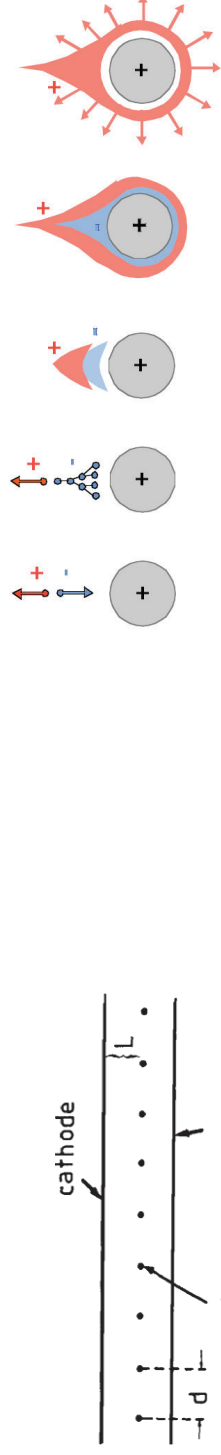
- 1) **camere a fili**: veloci, buona risoluzione spaziale ($\cong 0.3 - 0.5$ mm), self-triggering; informazione energia; usate in UA1 (Rubbia), fondamentali nella scoperta **W,Z0**.
- 2) **camere a deriva in gas**: coordinata pto passaggio basata su misura tempo raccolta della carica. Risoluzione spaziale $\cong 50 - 200$ μm
- 3) **TPC** (Camera a proiezione temporale): Camere deriva + proporzionali
- 4) **Camere a deriva in semiconduttori**: resa 3 eV per coppia; risoluzione spaziale $\cong 10$ μm .

Camere a fili: Multi wire proportional chambers

Varie tipologie:

- 1) **camere a fili:** veloci, buona risoluzione spaziale ($\cong 0.3 - 0.5 \text{ mm}$), self-triggering; informazione energia; usate in UA1 (Rubbia), fondamentali nella scoperta W, Z^0 .

(G. Charpak et al., Nobel prize 1992)



Letture digitale: la risoluzione spaziale e' limitata a:

$$\sigma_x \approx \frac{d}{\sqrt{12}}$$

$$(d=1\text{mm}, \sigma_x \approx 300 \mu\text{m})$$

Multi wire proportional chambers

Molti tracciatori (spettrometri,...) basati su camere a fili

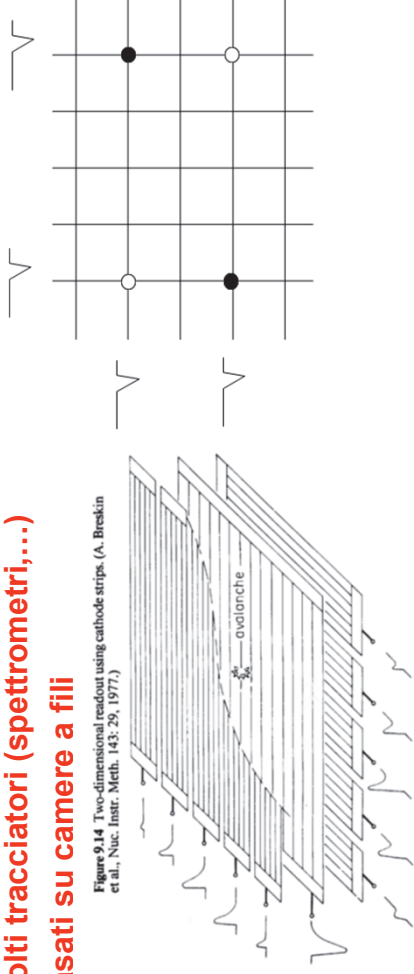
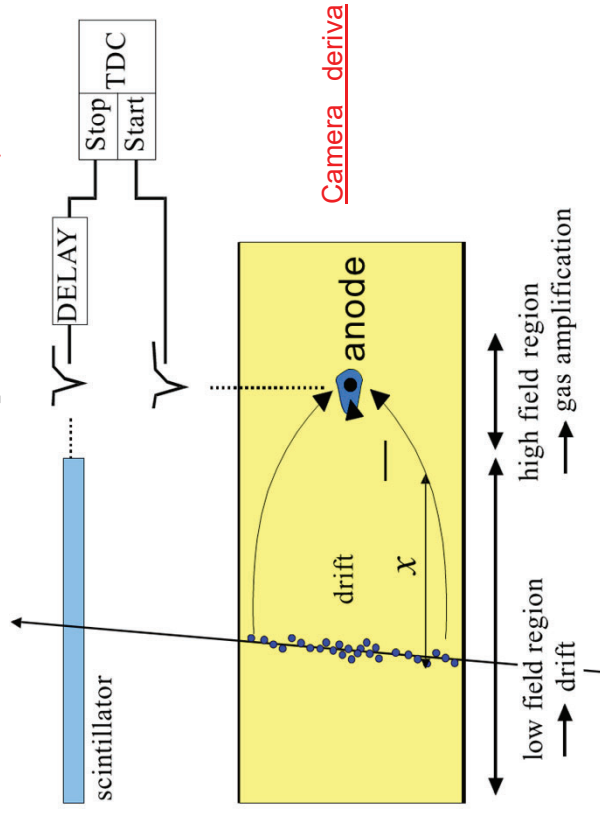


Figure 9.14 Two-dimensional readout using cathode strips. (A. Breskin et al., Nuc. Instr. Meth. 143: 29, 1977.)

2) **camera a deriva in gas**: coordinata pto passaggio basata su misura tempo raccolta della carica. Risoluzione spaziale \cong **50 – 200 μm**



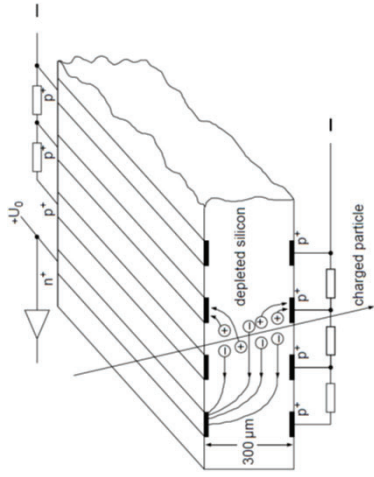
Camera deriva

- ◆ Misura il tempo di arrivo degli elettroni al filo a tensione relativo a t_0

$$x = \int v_D(t) dt$$

Camere a ionizzazione a semiconduttori:

3 eV per coppia; risoluzione spaziale $< \cong 10 \mu\text{m}$.



216

7 Track detectors

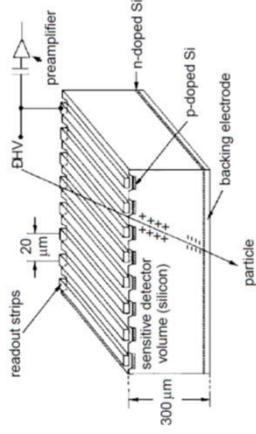
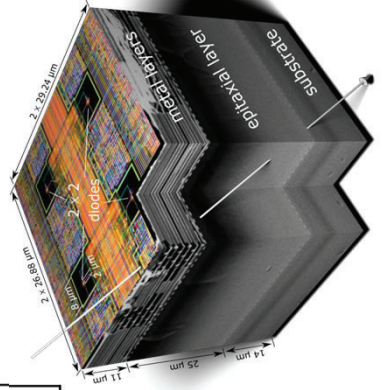
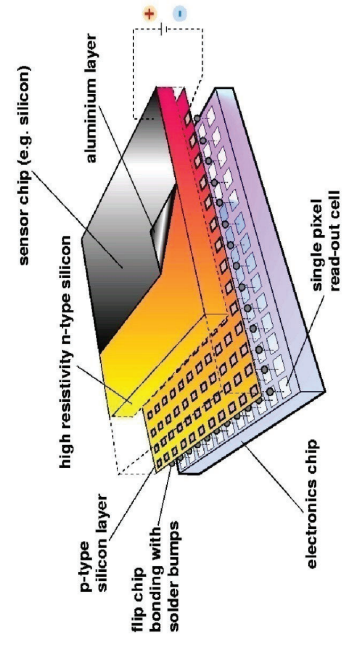
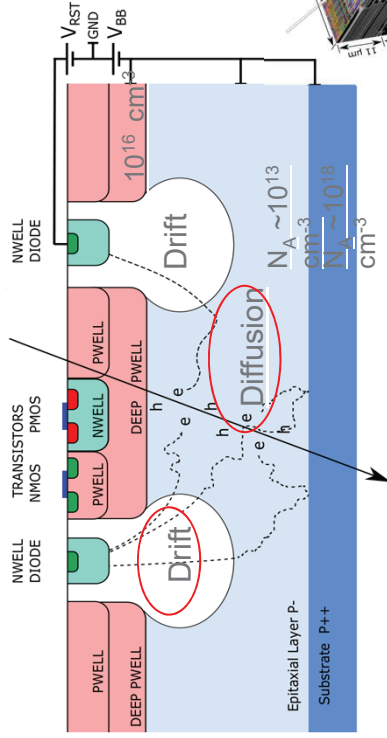


Fig. 7.39. Schematic layout of the construction of a silicon microstrip detector. Each readout strip is at negative potential. The strips are capacitively coupled (not to scale, from [103]).

Fig. 7.42. Silicon drift chamber with graded potential [100, 117–119].



TPC: Camere a proiezione temporale

TPC (Camera a proiezione temporale): Camere deriva + proporzionali
~("camera a nebbia elettronica")

Time Projection Chambers (TPC)

Large volume active detector.

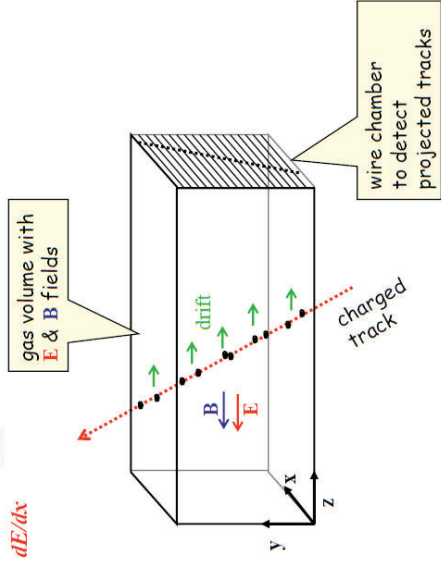
full 3-D track reconstruction

x - y from wires and segmented cathode of MWPC

z from drift time

and

dE/dx



TPC: Camere a proiezione temporale

TPC (Camera a proiezione temporale): Camere deriva + proporzionali
 ~("camera a bolle elettronica")

Time Projection Chambers (TPC)

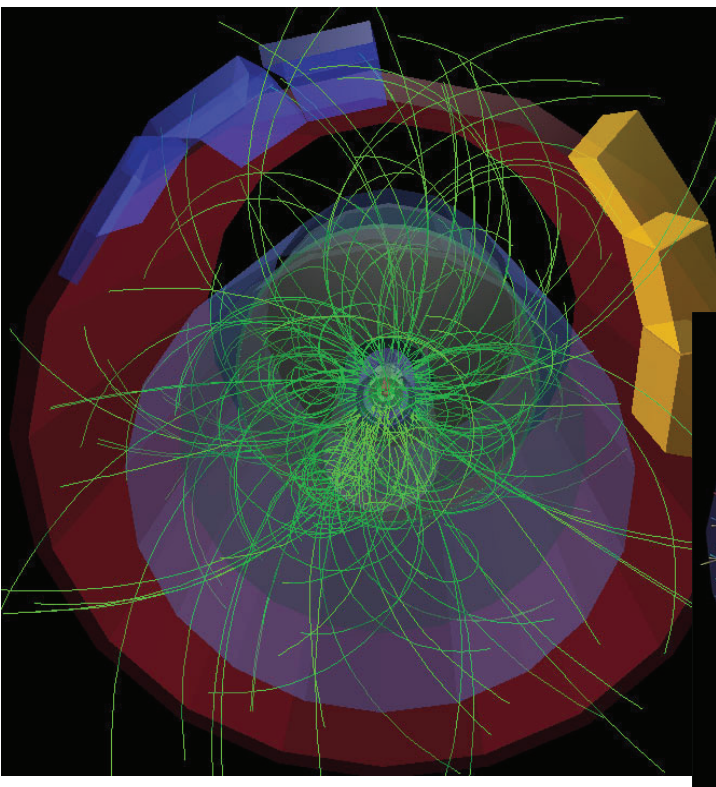
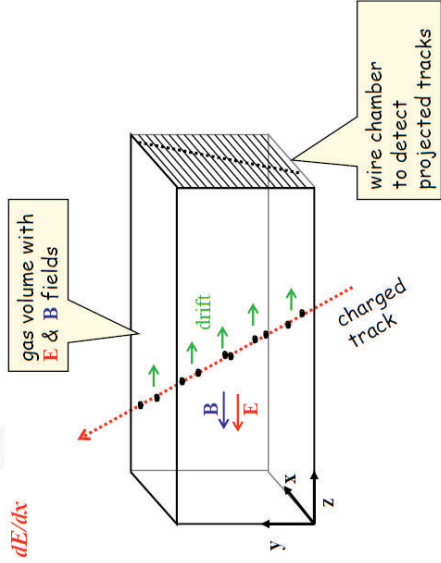
Large volume active detector.

full 3-D track reconstruction

x - y from wires and segmented cathode of MWPC

z from drift time

and dE/dx



Eventi ricostruiti dalla tpc di ALICE (L=5 m, diam=5m)

